

Maximizing the Grain Growth Rate during the Disorder-to-Order Transition in Block Copolymer Melts

W. G. KIM,¹ B. A. GARETZ,² M. C. NEWSTEIN,³ N. P. BALSARA⁴

¹Department of Physics, Polytechnic University, Six Metrotech Center, Brooklyn, New York 11201

²Department of Chemical Engineering, Chemistry, and Materials Science, Polytechnic University, Six Metrotech Center, Brooklyn, New York 11201

³Department of Electrical Engineering, Polytechnic University, Six Metrotech Center, Brooklyn, New York 11201

⁴Department of Chemical Engineering, University of California, Berkeley, California 94720.

Received 23 April 2001; revised 18 June 2001; accepted 20 June 2001

ABSTRACT: The factors controlling grain growth during the disorder-to-order transition in a polystyrene-*block*-polyisoprene copolymer melt were studied with time-resolved depolarized light scattering. The ordered phase consisted of hexagonally packed polyisoprene cylinders, and the order-disorder-transition temperature of the block copolymer (T_{ODT}) was 132 ± 1 °C. Our objective was to identify the temperature at which the grain growth rate was maximized (T_{max}) and compare it with theoretical predictions. We conducted seeded grain growth experiments, which comprised two steps. In the first step, which lasted for 43 min, the sample was cooled from the disordered state to 124 °C. This resulted in the formation of a small number of ordered grains or seeds. This was followed by a second step in which the sample was heated to temperatures between 124 and 132 °C and the seeds grew with time. Our objective was to study grain growth at different temperatures starting from the same initial condition. The value of T_{max} obtained experimentally was 128 °C. The theoretically predicted value of T_{max} , based entirely on the rheological properties of the disordered sample and T_{ODT} , was also 128 °C. © 2001 John Wiley & Sons, Inc. *J Polym Sci Part B: Polym Phys* 39: 2231–2242, 2001

Keywords: block copolymers; ordering kinetics; grain growth; light scattering

INTRODUCTION

There is considerable interest in quantifying the factors that control the growth rate of ordered grains after a quench from the disordered state. The temperature dependence of the growth rates

is sharply peaked at a temperature T_{max} because of the interplay between thermodynamic and frictional factors.^{1,2} At high temperatures or low quench depths ($T > T_{\text{max}}$), ordering kinetics are controlled by the weakness of the thermodynamic driving forces, and the rate of order formation thus increases with decreasing temperature. However, the frictional forces that resist molecular and collective motions necessary for order formation increase with rapidly decreasing temperature. In the $T < T_{\text{max}}$ temperature range, the rate of order formation is controlled by frictional resistance, leading to a decrease in the rate of order formation with decreasing temperature.

Contribution from the March 2001 Meeting of the American Physical Society—Division of Polymer Physics, Seattle, Washington.

Correspondence to: B. A. Garetz (E-mail: bgaretz@duke.poly.edu) or N. P. Balsara (E-mail: nbalsara@cchem.berkeley.edu)

Journal of Polymer Science: Part B: Polymer Physics, Vol. 39, 2231–2242 (2001)
© 2001 John Wiley & Sons, Inc.

The arguments for the existence of T_{\max} are quite general. It is, therefore, not surprising that T_{\max} has been identified in numerous classical solids that order with cooling, such as metals, ceramics, and crystalline polymers.^{1,2}

Explicit predictions of T_{\max} can be made if the temperature dependencies of the thermodynamic and frictional factors are known. Robust theories that describe the temperature dependence of molecular and collective motion in polymers are readily available.³ In contrast, equations for predicting the thermodynamic forces that drive order formation in polymers are often not available.

This article is concerned with the identification of T_{\max} for the disorder-to-order transition in block copolymer melts. An attractive feature of these materials is that the thermodynamic forces that drive order formation are well established.^{4–8} This enables explicit predictions of T_{\max} . Surprisingly, experimental studies on block copolymers indicate that the rate of order formation is a monotonic function of temperature. Rosedale and Bates⁹ followed the kinetics of the disorder-to-order transition in a poly(methylbutylene)-*block*-poly(ethylene) copolymer melt with time-resolved rheology and found that the kinetics slowed down monotonically with increasing temperature. Floudas et al.¹⁰ estimated the time required to complete the disorder-to-order transition in a polystyrene-*block*-polyisoprene copolymer melt by the same method and found the same result: slower kinetics at higher temperatures. This suggests that in both cases,^{9,10} the experiments were conducted at $T > T_{\max}$; that is, order formation was controlled by thermodynamic factors. This is surprising when one considers the fact that the experiments on the polystyrene-*block*-polyisoprene copolymer¹⁰ were conducted at temperatures between 74 and 86 °C. Under these conditions, frictional forces are expected to increase rapidly with decreasing temperature because of the proximity to the glass-transition temperature of the polystyrene chains. Time-resolved small-angle X-ray scattering (SAXS) measurements on polystyrene-*block*-polyisoprene copolymer melts also show slower kinetics at higher temperatures.¹¹

At least two parameters are necessary to characterize the structure of partially ordered block copolymers: the average volume of the ordered grains (v_g) and the volume fraction of the grains (ϕ). Ordering kinetics inferred from rheology are usually obtained from the time dependence of the in-phase shear modulus (G').^{9,10} Simple models suggest that G' is mainly a function of ϕ . Thus,

the kinetic measurements based on rheology reflect the time dependence of ϕ . Similarly, SAXS intensity is also proportional to ϕ .¹² It is thus conceivable that techniques sensitive to v_g may yield different results.

Our group has shown that time-resolved depolarized light scattering measurements enable the determination of both v_g and ϕ as a function of time.^{13–19} In a recent article,¹⁸ we used this technique to study grain growth in a quenched polystyrene-*block*-polyisoprene copolymer melt. The time required for ϕ to reach unity increased monotonically with decreasing temperature, a result that is consistent with previous work.^{9–11} In contrast, the measured grain growth rate (dv_g/dt during the early stages of the disorder-to-order transition) decreased monotonically with decreasing temperature.¹⁸ We argued that these results were obtained because ordering kinetics in our sample were dominated by nucleation effects.¹⁸

The main purpose of this article, which is a continuation of the work described in ref. 18, is to identify the factors that control grain growth rates in block copolymers. This can only be accomplished if growth rates are studied at a fixed nucleation density. We begin by presenting the equations that enable the explicit prediction of T_{\max} in block copolymers. This is followed by an experimental test of the prediction.

THEORETICAL PREDICTION OF T_{\max}

The theory of Goveas and Milner⁷ predicts that the velocity with which the ordered front propagates into the disordered phase during a disorder-to-order transition (v) is given by

$$v = \frac{RN}{\tau} [\chi - \chi_{\text{ODT}}] g(f) \quad (1)$$

Equation 1 applies to an A–B diblock copolymer with N repeat units, fN of which are type A and $(1-f)N$ of which are type B. In eq 1, R is the end-to-end distance of the copolymer, τ is the characteristic relaxation time, χ is the Flory–Huggins interaction parameter, χ_{ODT} is the Flory–Huggins interaction parameter at the order–disorder-transition temperature (T_{ODT}), and $g(f)$ is an order unity constant that depends only on f . For most pairs of polymers, χ is a linear function of $1/T$:

$$\chi = A + B/T \quad (2)$$

where T is the absolute temperature. The temperature dependence of the longest relaxation time in polymers is often described by the Williams–Landel–Ferry (WLF) equation:

$$\log\left(\frac{\tau}{\tau_{\text{ref}}}\right) = -\frac{C_1(T - T_{\text{ref}})}{C_2 + (T - T_{\text{ref}})} \quad (3)$$

In eq 3, τ_{ref} is the characteristic relaxation time at a reference temperature (T_{ref}) that can be chosen arbitrarily. Setting T_{ref} equal to T_{ODT} and substituting eqs 2 and 3 into 1 give

$$v = v_0 \frac{1/T - 1/T_{\text{ODT}}}{10^{-C_1(T - T_{\text{ODT}})/(C_2 + T - T_{\text{ODT}})}} \quad (4)$$

where v_0 , given by

$$v_0 = \frac{RNBg(f)}{\tau_{\text{ref}}} \quad (5)$$

is a weak function of temperature. T_{max} can thus be predicted with eq 4 if C_1 , C_2 , and T_{ODT} are known.

It is important to recognize that the theory of Goveas and Milner assumes that nucleation barriers have been overcome. It is, therefore, necessary to ensure that the experiments are conducted under these conditions.

EXPERIMENTAL

The polystyrene-*block*-polyisoprene copolymer used in this study was also used in ref. 18. The weight-average molar masses of the polystyrene and polyisoprene blocks were determined to be 19.8 and 6.0 kg/mol, respectively, and the polydispersity index of the copolymer was 1.07. We refer to this polymer as SI(20-6). The volume fraction of polyisoprene in the block copolymer is 0.26. On the basis of extensive characterization of polystyrene-*block*-polyisoprene copolymers,²⁰ we expect the sample to have a cylindrical microstructure at temperatures of interest, 124–132 °C. All of our experiments were conducted well above the spinodal temperature, which was estimated to be 87 °C.¹⁸ The glass-transition temperature of the polystyrene-rich microphase was measured with differential scanning calorimetry experiments

conducted on an ordered sample and was determined to be 78 °C.

Depolarized light scattering experiments were conducted on 1-mm-thick SI(20-6) melts enclosed between optical flats. Details concerning the instrumentation and data analysis are given in ref. 18. A beam of light from a 15-mW He–Ne laser ($\lambda = 633$ nm) was directed through a polarizer before it reached the sample, which was housed in a thermostated oven. The scattered light transmitted through the sample passed through an analyzer whose optic axis was perpendicular to the polarizer and was projected onto a screen. We define μ to be the azimuthal angle in the scattering plane relative to the direction of the analyzer axis. The polar angle between the incident and scattered rays emanating from the sample is θ . The depolarized scattering intensity I was recorded as a function of θ along two azimuthal angles, $\mu = 0^\circ$ and $\mu = 45^\circ$. We report I as a function of the scattering vector q [$q = 4\pi\sin(\theta/2)/\lambda$].

Small-angle neutron scattering (SANS) experiments were conducted on the NG3 beamline at the National Institute of Standards and Technology (Gaithersburg, MD), as described in ref. 18. Rheological measurements, described in ref. 18, were conducted on an ARES instrument built by Rheometrics Scientific in a dry nitrogen environment, with 25-mm-diameter parallel-plate fixtures and a transducer with a dynamic range of 200–0.2 g · cm.

The parameters B , R , N , τ_{ref} , C_1 , C_2 , and T_{ODT} , required to predict grain growth rates in SI(20-6) were obtained from independent experiments. B and R were obtained with SANS; N was obtained from polymer characterization; τ_{ref} , C_1 , and C_2 were determined from rheological studies; and T_{ODT} was determined with depolarized light scattering.

THEORETICAL MODEL FOR THE INTERPRETATION OF DEPOLARIZED LIGHT SCATTERING DATA

We provide a brief summary of the equations that describe depolarized light scattering from ordered block copolymers. The model used in this work was developed in refs. 16 and 19, and data analysis details are reported in ref. 18. We assume that the sample is composed of randomly oriented ordered grains coexisting with disordered regions. The volume fraction of the ordered grains is ϕ . Each grain is a birefringent, uniaxial crystal with

an optic axis parallel to the cylinder axis. The scattered field from this collection of grains is determined by the probability that given a point inside a grain with the optic axis along a unit vector \mathbf{g} , a vector \mathbf{R} emanating from that point lies entirely within that grain. We assume that this probability distribution $C(\mathbf{R}, \mathbf{g})$ is of the Gaussian ellipsoidal form:

$$C(\mathbf{R}, \mathbf{g}) = \exp\left(-\frac{1}{2}\left(\frac{\mathbf{a} \cdot \mathbf{R}}{w}\right)^2\right) \times \exp\left(-\frac{1}{2}\left(\frac{\mathbf{b} \cdot \mathbf{R}}{w}\right)^2\right) \exp\left(-\frac{1}{2}\left(\frac{\mathbf{g} \cdot \mathbf{R}}{l}\right)^2\right) \quad (6)$$

where $\{\mathbf{g}, \mathbf{a}, \mathbf{b}\}$ are an orthogonal set of unit vectors. The characteristic lengths of the ellipsoidal grains in the directions parallel and perpendicular to the optic axis are l and w , respectively. The scattering profiles $I(q, \mu)$ for such a system along the $\mu = 0$ and 45° directions is given by

$$I(q, 0^\circ) = I_0[C(q) + D(q)] \quad (7)$$

and

$$I(q, 45^\circ) = I_0[C(q) - D(q)] \quad (8)$$

where

$$C(q) = \frac{15}{16} \exp\left[-\frac{q^2 w^2}{2}\right] \int_0^\pi d\alpha \sin^5 \alpha \times \exp[-\beta(\alpha)] I_{m0}[\beta(\alpha)] \quad (9)$$

and

$$D(q) = -\frac{15}{16} \exp\left[-\frac{q^2 w^2}{2}\right] \int_0^\pi d\alpha \sin^5 \alpha \times \exp[-\beta(\alpha)] I_{m2}[\beta(\alpha)] \quad (10)$$

$\beta(\alpha) = (q^2 l^2 / 4)[1 - w^2 / l^2] \sin^2 \alpha$, I_{mj} is the modified Bessel function of order j , and

$$I_0 = K_c (\Delta n)^2 w^2 l \phi = K_c (\Delta n)^2 v_g \phi \quad (11)$$

where K_c is an instrumental constant and $v_g = w^2 l$ is the characteristic grain volume. The average number of ordered grains per unit volume (ρ) is given by

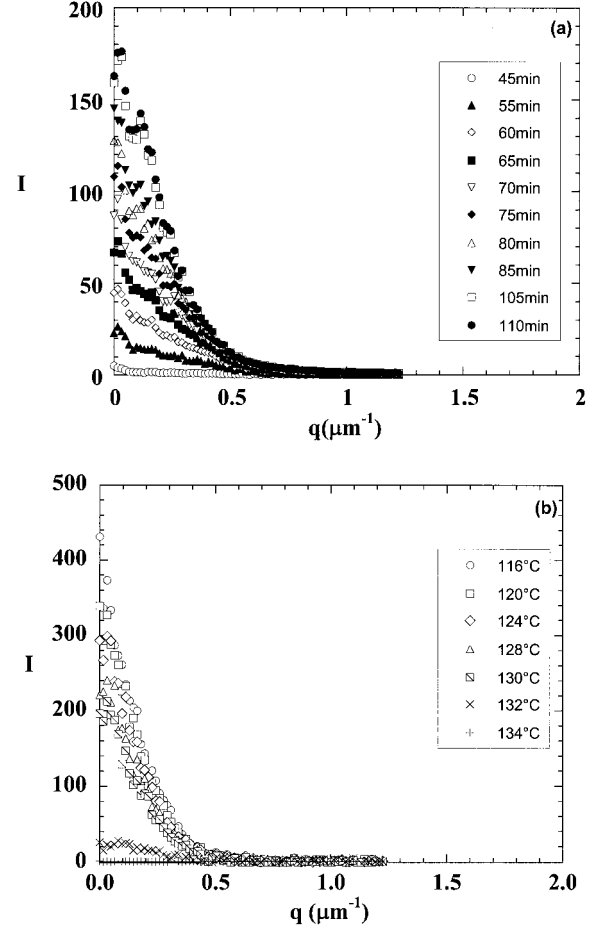


Figure 1. I versus q along the $\mu = 45^\circ$ direction: (a) at selected times after quenching from the disordered state to 124°C and (b) as a function of increasing temperature. $I(q)$ is negligible at 134°C , indicating that T_{ODT} is $133 \pm 1^\circ\text{C}$.

$$\rho = \phi / v_g. \quad (12)$$

RESULTS AND DISCUSSION

The SI(20-6) melt was first heated to 145°C (well above T_{ODT}), and then it was cooled to 124°C . Time zero is defined as the time at which the temperature controller setting was changed from 145 to 124°C . It took about 40 min for the sample temperature to be within 1°C of the final temperature. The sample was held at 124°C until $t = 110$ min. The results of this experiment are given in Figure 1(a), where we show $I(q, \mu = 45^\circ)$ as a function of time. At $t = 45$ min, we see a small but noticeable depolarized light scattering signal indicating the start of the disorder-to-order tran-

sition. The signal saturates around $t \approx 100$ min, indicating the completion of the disorder-to-order transition.

The sample was then cooled to 116 °C and studied as a function of increasing temperature. The sample was kept at each temperature for 30 min before the data were taken. The results of this experiment are shown in Figure 1(b), where scattering profiles [$I(q, \mu = 45^\circ)$] at selected temperatures are shown. The depolarized light scattering signal decreases with increasing temperature. We assume that the temperature jump that results in complete extinction of the depolarized light scattering signal gives the order-to-disorder transition.^{13,14} We thus conclude that T_{ODT} is 133 ± 1 °C [Fig. 1(b)].

We then conducted experiments in which the order formation in SI(20-6) was conducted in two steps. The sample was disordered at 145 °C at the beginning of each experiment and then cooled to 124 °C. At $t = 43$ min, after the disorder-to-order transition had been initiated at 124 °C, the sample was subjected to a second step, in which the sample temperature was increased to 126 °C. It took about 1 min to change the sample temperature from 124 to 126 °C. The result of this experiment is shown in Figure 2(a). A relatively weak signal at $t = 45$ min indicates that a small fraction of the sample is converted into ordered grains at the beginning of the second step. We thus refer to the ordered grains formed during the first step as seeds. It is evident from Figure 2(a) that the depolarized signal increases by two orders of magnitude during the second step, indicating that most of the growth of the ordered grains occurs during this step. We thus refer to the first step as the seeding step and the second step as the growth step. Our two-step experiments can be thus regarded as seeded grain growth experiments.

We conducted a series of seeded grain growth experiments, keeping the seeding step fixed. Thus, in all cases we began by disordering the sample, quenching the sample to 124 °C, and keeping the sample at 124 °C until $t = 43$ min. The temperature of the growth step was varied from 124 to 133 °C. These experiments enable a study of grain growth at different temperatures, with the same initial conditions (seeds). We focused on growth temperatures above the seeding temperature to minimize the formation of additional nuclei during the growth step. We refer to each seeded growth experiment by the temperature of the growth step. In Figure 2(b–e), we show

$I(q, \mu = 45^\circ)$ data obtained during seeded grain growth at 128, 130, 132, and 133 °C, respectively. When the temperature of the growth step is less than equal to 132 °C, we see irreversible grain growth after the seeding step. This is indicated by the rapid increase in I seen in Figure 2(a–d). The scattered intensity at the lowest accessible q increases by a factor of 20 or larger in the $45 \text{ min} < t < 100 \text{ min}$ range. At a growth temperature of 133 °C, we do not observe irreversible growth of the ordered phase. As can be seen in Figure 2(e), the value of I at the lowest accessible q value [$I(q = 0.1 \mu\text{m}^{-1})$] was about 2 units at $t = 45$ min (after the seeding step). When the growth step was executed, $I(q = 0.1 \mu\text{m}^{-1})$ increased initially to about 4 units. However, with time the scattered intensity decreased, indicating dissolution of the seeds. The dissolution kinetics occur very slowly, indicating that the system at 133 °C is close to the equilibrium order-disorder transition temperature. This result, which is based on grain growth in a sample with a small concentration of ordered seeds, is entirely consistent with the assignment of $T_{\text{ODT}} = 133 \pm 1$ °C, which was based on disordering a fully ordered sample [Fig. 1(b)]. There is thus no evidence of hysteresis in the order-disorder transition in SI(20-6), provided the sample is seeded at 124 °C.

In Figure 3, we show typical scattering profiles $I(q)$ along $\mu = 0$ and 45° obtained during the growth step. In Figure 3(a), we show early time ($t = 50$ min) data, whereas in Figure 3(b), we show the late time data ($t = 100$ min); both data sets are taken from the 130 °C seeded grain growth experiments [Fig. 2(c)]. Our method for data analysis is identical to that described in detail in ref. 18. The dashed and solid curves in Figure 3 are fits of eqs 7 and 8 through the $\mu = 0$ and 45° data, respectively, with l , w , and I_0 as adjustable parameters. The theoretical scattering curves were computed over a wide range of l , w , and I_0 values. The sum of the square of the deviation between the theoretical and experiment I , $(\Delta I)^2$, over the entire range of q and μ were computed for each combination of l , w , and I_0 . The combinations that gave the smallest average value of $|\Delta I|/I_0$ are reported in this article. All of the scattering profiles obtained during the seeded growth experiments were analyzed by this method. [For brevity, we only show $I(q, \mu = 45^\circ)$ data in most cases. For the data analysis, however, both $\mu = 0$ and $\mu = 45^\circ$ data were used.] We thus obtained the time dependence of I_0 , l , and w at different growth temperatures.

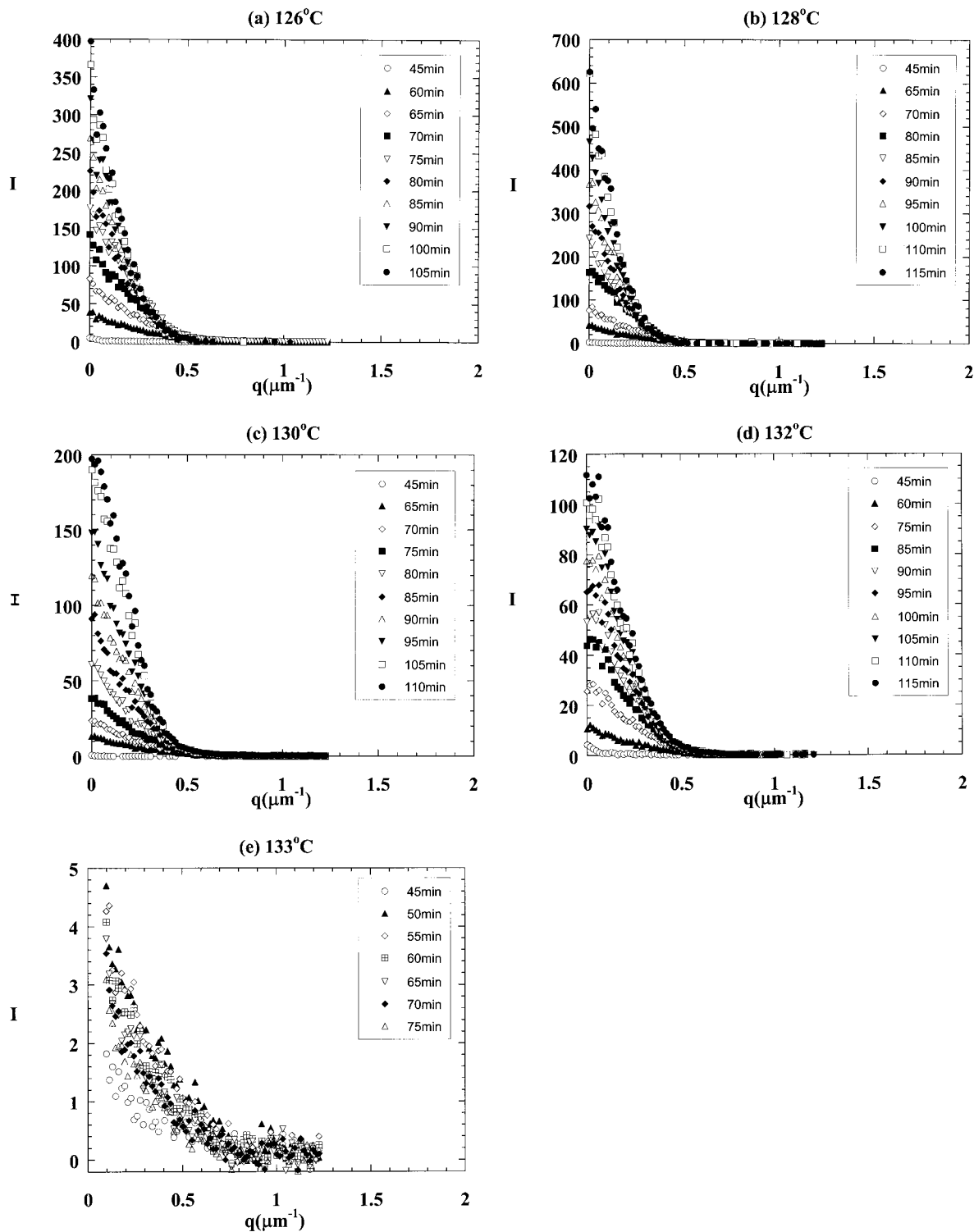


Figure 2. I versus q along the $\mu = 45^\circ$ direction during a series of seeded grain growth experiments. In each experiment, seeds for order formation were grown by the quenching of the sample from the disordered state to 124°C . The second step (i.e., the growth step) was started at $t = 45$ min. The temperatures used during the growth step were (a) 126°C , (b) 128°C , (c) 130°C , (d) 132°C , and (e) 133°C .

The time dependence of I_0 at different growth temperatures is shown in Figure 4. At early times ($t \leq 55$ min), I_0 values obtained at different growth temperatures are similar. This is expected because the same seeding step was used to initiate order formation in all of the experiments. At long times, I_0 values obtained at different growth temperatures are substantially different. The rate of increase of I_0 can be taken as a measure of the kinetics of the ordering process because $I_0 \propto \phi v_g$ (eq 11). Because all of the data sets of I_0 versus t start at the same value, the value of I_0 at some fixed later time is a convenient measure of the rate of increase of I_0 . Using I_0 at $t = 100$ min as a gauge of the ordering kinetics, we conclude that order formation is relatively slow at 124 °C, at which temperature $I_0(t = 100 \text{ min})$ is 150 units

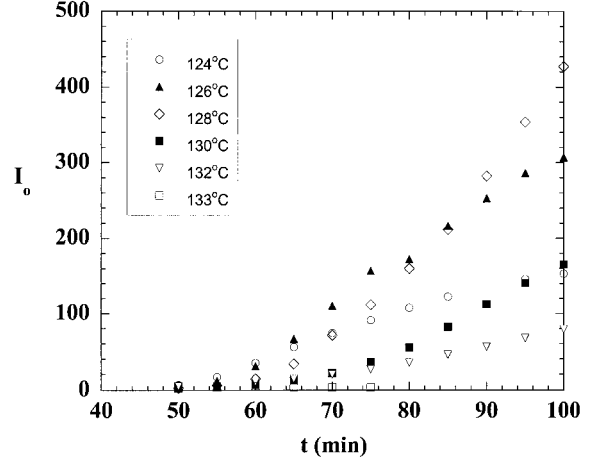


Figure 4. Time dependence of I_0 during seeded grain growth at different grain growth temperatures.

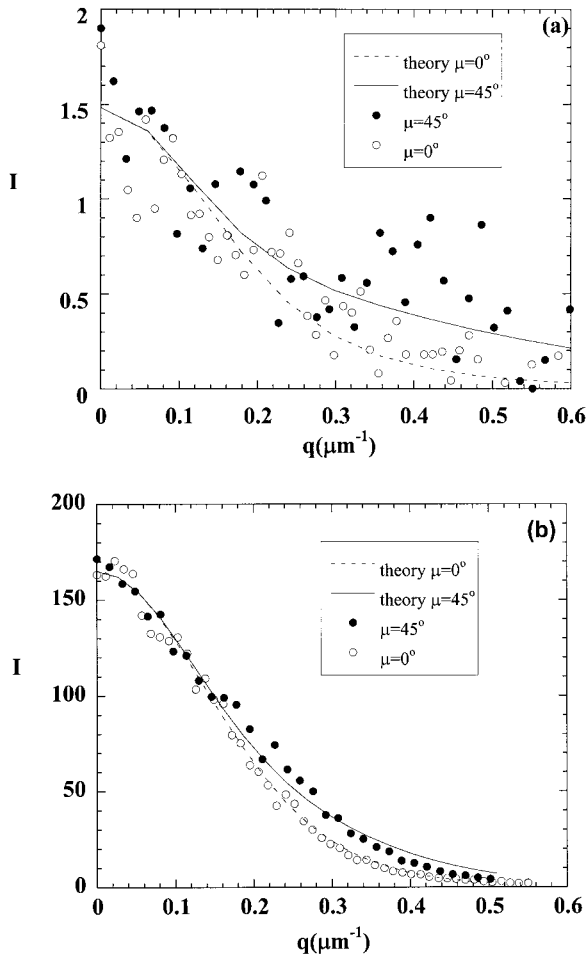


Figure 3. Typical depolarized light scattering profiles $[I(q)]$ along the $\mu = 0$ and 45° directions obtained during the seeded grain growth experiments: (a) $t = 50$ min and (b) $t = 100$ min. The curves are theoretical fits (eqs 7 and 8) with l , w , and I_0 as adjustable parameters.

(Fig. 4). Order formation becomes more rapid as the growth temperature is increased: at 126 °C, $I_0(t = 100 \text{ min})$ is 300 units, whereas at 128 °C, $I_0(t = 100 \text{ min})$ is 470 units. However, a further increase in the growth temperature leads to slower order formation: at 130 °C, $I_0(t = 100 \text{ min})$ is 160 units, whereas at 132 °C, $I_0(t = 100 \text{ min})$ is 80 units. We thus see the first indication of a non-monotonic temperature dependence of ordering kinetics in SI(20-6), suggesting that T_{max} is 128 °C.

The time dependencies of grain lengths l and w at different growth temperatures are shown in Figure 5(a,b), respectively. The time dependence of l and w at early times can be approximated by straight lines; the lines in Figure 5 are least-squares fits through the $t < 80$ min data. At longer times, substantially slower growth rates are obtained because of the increasing influence of neighboring grains.^{15,16} The slope of the lines in Figure 5 give the initial grain growth velocity along the optic axis and perpendicular to it: $v_1 = dl/dt$ and $v_w = dw/dt$. We focus on the initial velocity because eq 4 was derived for the case of an isolated ordered front propagating into a disordered phase.⁷

The temperature dependence of the rheological relaxation time τ in disordered SI(20-6) melts was estimated from rheological measurements, as described in ref. 18. The results are shown in Figure 6, where τ/τ_{ref} is plotted as a function of temperature. The value of τ_{ref} at $T_{\text{ref}} = T_{\text{ODT}} = 133 \text{ °C}$ was 0.009 s.¹⁸ It is evident that to a good approximation, the temperature dependence of τ can be represented by the WLF equation (eq 3). The line in Figure 6 is a least-squares fit of eq 3, which

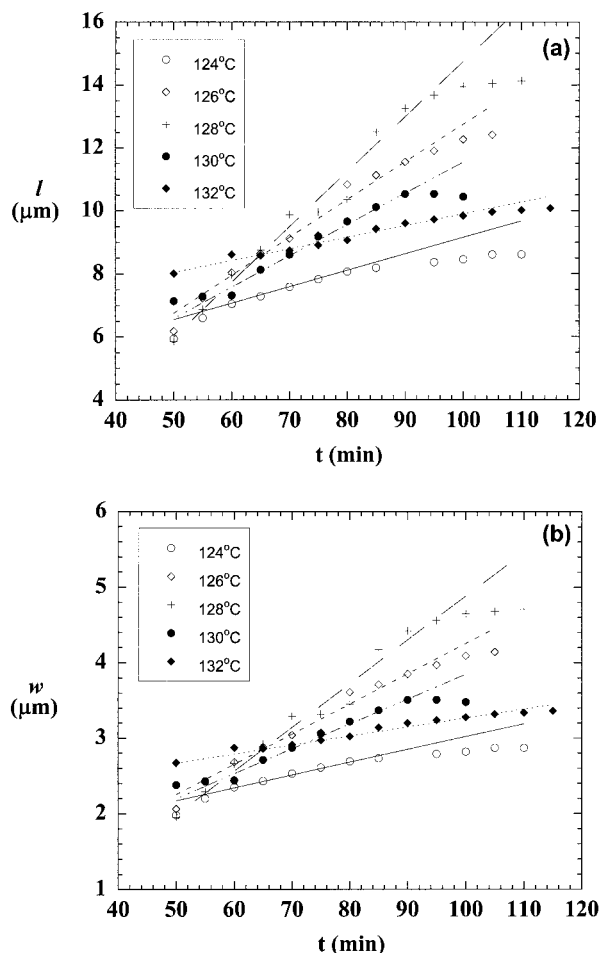


Figure 5. Time dependence of the average grain size during seeded grain growth experiments at different grain growth temperatures: (a) l and (b) w .

gives $C_1 = 14.10$ (K) and $C_2 = 161.2$ (K). We estimate τ is the ordered state ($T < T_{\text{ODT}}$) by extrapolating the WLF curve shown in Figure 6. Some justification for this is provided in ref. 17. For the SI block copolymer sample used in ref. 17, there were no detectable signatures of order formation for $t < 100$ min. This enabled the rheological characterization of the metastable disordered state at $T < T_{\text{ODT}}$. It was found that the measured values of τ were in excellent agreement with WLF extrapolations from the disordered state. In SI(20-6), order formation begins rapidly in the temperature range of interest, thus precluding rheological characterization of the metastable disordered state at $T < T_{\text{ODT}}$.

In Figure 7, we show the temperature dependence of the grain growth velocities v_l and v_w . The symbols and dashed lines represent the experimentally determined grain growth rates. The

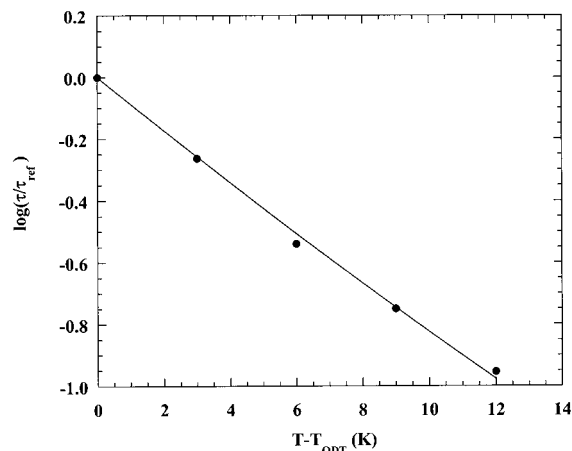


Figure 6. Temperature dependence of the rheological relaxation time τ of SI(20-6). The line is the least-squares WLF fit (eq 3).

solid curves in Figure 7 are plots of eq 4 with the previously given parameters C_1 , C_2 , and T_{ODT} . Theory and experiment are in remarkable agreement; both indicate that T_{max} for SI(20-6) is 128 °C. There is, however, a considerable difference in the shapes of the experimental and theoretical curves in Figure 7. We adjusted the parameter v_0 in eq 4 to obtain agreement with the experimentally determined grain growth velocity at 128 °C.

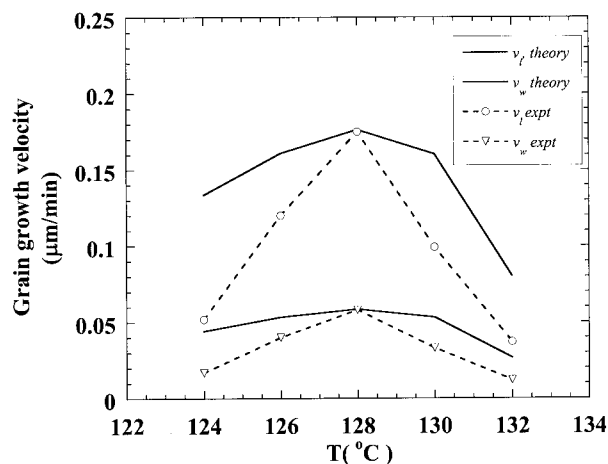


Figure 7. Temperature dependence of the experimentally determined grain growth velocities during seeded grain growth (v_l and v_w) compared with the theory of Goveas and Milner (eq 4). The dashed lines are guides to the eye. Both theory and experiment indicate that T_{max} is 128 °C. We adjusted the value of v_0 in eq 4 to obtain agreement at T_{max} . The theory does not address anisotropic grain growth, that is, differences in v_0 along different directions.

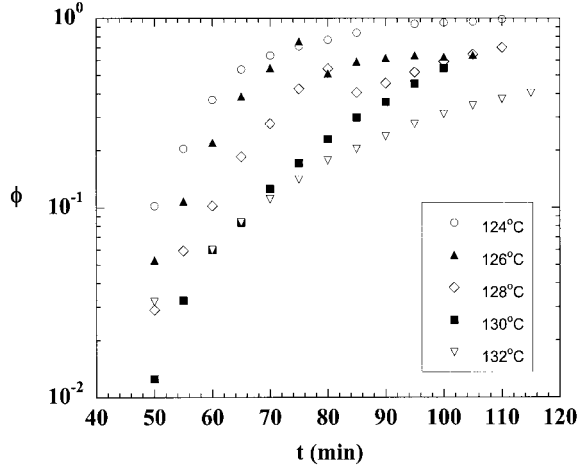


Figure 8. Time dependence of ϕ during seeded grain growth at different grain growth temperatures.

Despite this adjustment, the shapes of the theoretical and experimental curves are quite different. The experimentally observed peak in grain growth rates is much sharper than theoretical predictions (Fig. 7). This indicates that some aspects of our experiments are not captured by the theory. Additional doubts regarding the agreement between theory and experiment arise when one examines the theoretical and experimental values of the prefactor v_0 . All of the parameters in eq 5 have been measured: $R = 0.0132 \mu\text{m}$ (based on SANS data presented in ref. 18; the scattering peak at T_{ODT} was located at $q_{\text{peak}} = 0.38 \text{ nm}^{-1}$ and $R = 5.007/q_{\text{peak}}$ for a block copolymer with $f = 0.26$; see ref. 4), $N = 300$ (polymer characterization), $B = 20.0 \text{ K}$ (ref. 21), and $g(f) = 0.575$ (ref. 17). The N and B values are based on a reference volume of 150.3 \AA^3 . The theoretical value of v_0 is thus $3.04 \times 10^5 \text{ K } \mu\text{m}/\text{min}$. The values of v_0 used to match theory and experiment in Figure 7 are much lower: $1.61 \times 10^4 \text{ K } \mu\text{m}/\text{min}$ for matching v_1 and $5.34 \times 10^3 \text{ K } \mu\text{m}/\text{min}$ for matching v_w . In other words, the grain growth velocities that we have measured are about an order of magnitude smaller than those predicted by the Goveas and Milner theory. One of the assumptions of the theory is that grains grow via the incorporation of individual molecules. In contrast, we concluded in ref. 18 that order formation in SI(20-6) requires the concerted motion of several (ca. 10^2) molecules. Perhaps the discrepancy between theoretical and experimental v_0 values is due to this difference. Definitive resolution of this discrepancy will require designing experiments that directly probe the molecular events that lead to order formation.

Another possible reason for the discrepancy in v_0 values is revealed when we examine the time dependence of ϕ and ρ during our seeded grain growth experiments. We assume that $\phi = 1$ during the late stage ($t = 110 \text{ min}$) of the 124°C growth step [Fig. 1(a)]. Equation 11 allows us to calculate the product $K_c \Delta n^2$ with the experimentally determined values of I_0 and v_g at $t = 110 \text{ min}$. We find that $K_c \Delta n^2 = 2.4$. In ref. 18, we showed that Δn was a weak function of temperature; it changed by 10% in the temperature range of interest. A simple expression for the time dependence of ϕ in terms of measured quantities ($v_g = lw^2$ and ϕ) is obtained if we ignore this change in Δn :

$$\phi = \frac{I_0}{2.4v_g} \quad (13)$$

The time dependence of ϕ at different growth temperatures is shown in Figure 8.²² It is evident that ϕ is less than or equal to 0.1 at $t = 50 \text{ min}$, regardless of growth temperature. The initial value of ϕ for all of the seeded growth experiments is thus similar. However, in the time window between $t = 50 \text{ min}$ and $t = 80 \text{ min}$, ϕ increases rapidly. Note that our estimates of grain growth velocities (Fig. 5) were obtained during this time interval. At $t = 80 \text{ min}$, ϕ ranges from 0.2 to 0.8, depending on the temperature of the growth step. Thus, the grain growth velocities that we have measured are affected by the presence of neighboring grains.

In Figure 9, we plot the time dependence of the

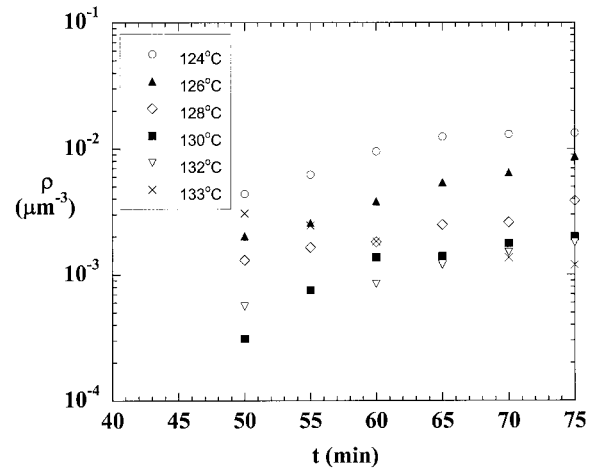


Figure 9. The nucleation density (ρ_{nucl}) versus time during seeded grain growth at different grain growth temperatures.

grain density ρ ($\rho = \phi/v_g$) during the growth step. Our seeded grain growth experiments were designed to study grain growth under identical nucleation conditions. If our experiments had worked perfectly, ρ would be independent of time and temperature. Figure 9 shows that our experiments are far from perfect: we find that substantial changes in ρ occur during the early stages of the growth step, that is, $45 \text{ min} < t < 50 \text{ min}$ (see Fig. 9). This is probably due to the extreme sensitivity of the nucleation process to thermal history.¹⁸ In addition, ρ increases with time during the growth step (Fig. 9). This could be due to the birth of new grains during the growth step (continuous nucleation) or the breakup of existing grains due to factors such as internal stresses within the grains or collisions with neighboring grains or secondary nucleation. We note that similar effects have been seen during the growth of colloidal crystals.²³ The theory presented in this article does not account for these events.

In Figure 10, we show grain growth kinetics obtained after direct cooling to the temperature of interest, that is, one-step grain growth experiments without the seeding step. These data are taken from ref. 18. The lines through the data indicate least-squares linear fits through the early time data ($t < 80 \text{ min}$), which give the grain growth velocities v_l and v_w . In Figure 11, we compare grain growth velocities obtained during seeded grain growth with those obtained in the absence of seeding. At 124°C , the seeded grain growth experiment is identical to a one-step experiment; the seeding and growth temperatures are both 124°C . Thus, the agreement seen in Figure 11 at 124°C only shows the reproducibility of our experiments. At temperatures less than T_{max} (128°C), the agreement between seeded and unseeded growth is quite good. The most dramatic differences between the seeded and unseeded growth experiments are observed at temperatures above T_{max} . The seeded experiments show clear evidence of critically slowed growth kinetics as the temperature approaches T_{ODT} , whereas the unseeded growth rates continue to increase with increasing temperature. At 130°C , v_l obtained during the unseeded experiments is $0.25 \mu\text{m}/\text{min}$, whereas v_l obtained during the seeded experiment is $0.10 \mu\text{m}/\text{min}$ (Fig. 11). The main difference between the seeded and unseeded experiments is the grain density ρ . In the unseeded experiment at 130°C , ρ at early times ($t = 65 \text{ min}$) is $2.0 \times 10^{-5} \mu\text{m}^{-1}$ based on ϕ and v_g values given in ref. 18. This is about 2 orders of

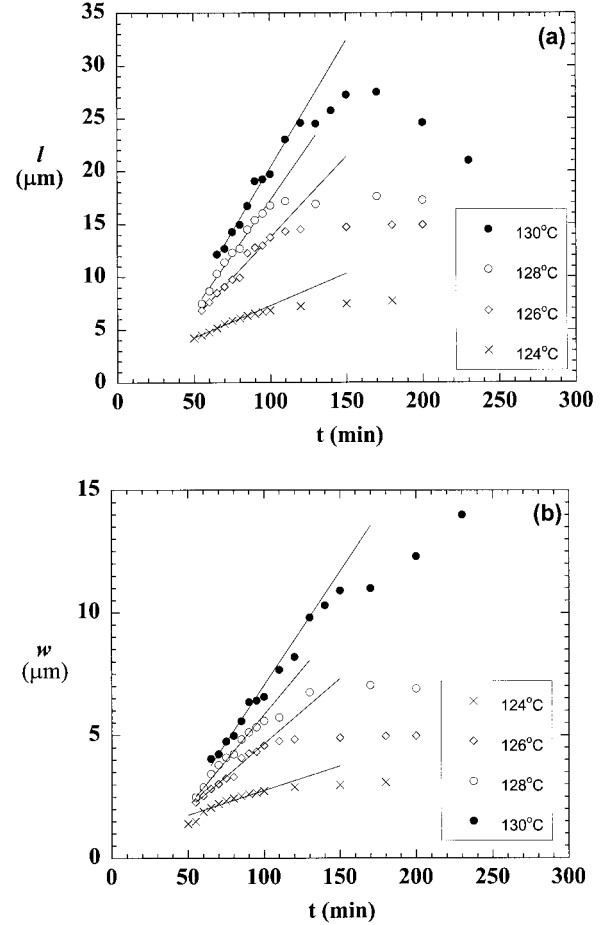


Figure 10. Time dependence of the average grain size during one-step ordering experiments at different grain growth temperatures (data from ref. 18): (a) l and (b) w .

magnitude lower than that obtained in the early stages of the seeded experiment, where $\rho = 3 \times 10^{-3} \mu\text{m}^{-1}$ at $t = 50 \text{ min}$. It is thus evident that lower values of ρ lead to higher grain growth rates. This provides a partial explanation for the discrepancy between theoretical and experimental values of v_0 reported previously. If we were able to measure grain growth rates at lower values of ρ , the agreement between experimental and theoretical values of v_0 would be better. However, designing such experiments is not straightforward because the factors that control ρ have not been identified. At 132°C , the unseeded grain growth velocity could not be measured [Fig. 11(a,b)]. At this temperature, the thermodynamic driving forces for order formation are so weak that order formation does not occur on experimental timescales in the absence of seeds [see Fig. 2(a) in ref. 18]. In contrast, irreversible grain

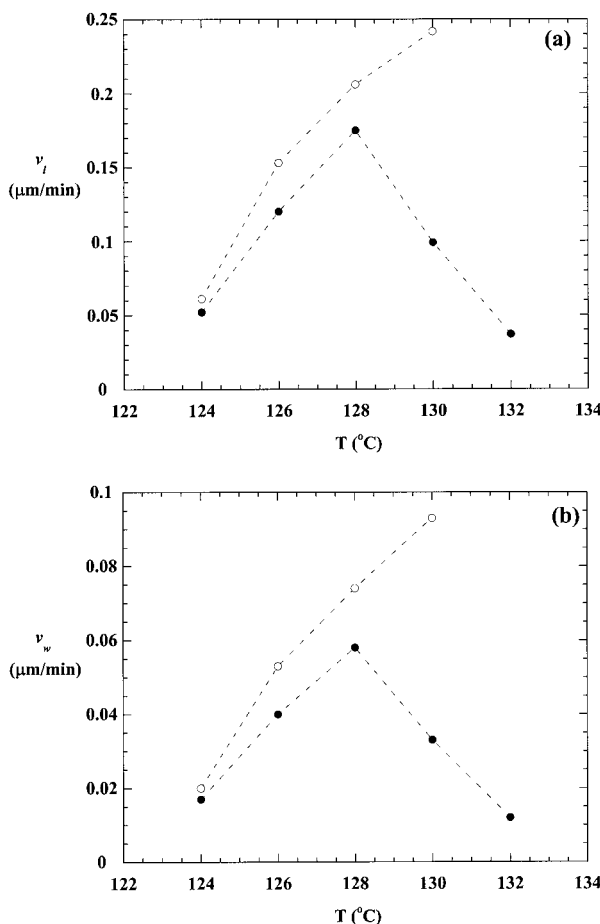


Figure 11. Comparison of the grain growth velocities obtained during seeded growth (filled circles) and those obtained in the absence of seeds (unfilled circles): (a) v_i versus T and (b) v_w versus T .

growth is seen at the same temperature (132 °C) during seeded grain growth [Fig. 11(a,b)].

CONCLUSIONS

The factors that control grain growth during the disorder-to-order transition in SI(20-6) were determined by a combination of depolarized light scattering, rheology, and SANS. Our objective was to identify T_{\max} , the temperature at which the grain growth rate is maximized. We conducted two-step ordering experiments in an attempt to accomplish our objective. The first step, in which the sample was cooled to 124 °C, resulted in the formation of a small number of ordered grains or seeds. This was followed by a second heating step to temperatures between 124 and 132 °C, in which the growth of grains was

studied. The temperature at which grain growth rates were maximum was 128 °C. This result is in excellent agreement with theoretical predictions. There is no hysteresis near the order-disorder transition in SI(20-6): measurable grain growth rates were obtained 1 °C below T_{ODT} after seeding. This makes block copolymers model materials for fundamental studies of ordering kinetics. Block copolymer are also convenient because of the availability of (1) well-established synthetic procedures, (2) a variety of experimental tools for studying grain growth, and (3) quantitative theoretical models that address the thermodynamics and kinetics of order formation.

Crystallization is the most widely studied disorder-to-order transition in polymeric systems.¹ It is perhaps appropriate to distinguish polymer crystallization and order formation in block copolymers. Unlike conventional three-dimensional crystals, the ordered phase that we have studied is liquid-crystalline; the crystalline order is restricted to two dimensions. Typical peaks in the temperature dependence of spherulite growth velocity reported in the literature¹ are much sharper than those reported here for block copolymers. This is due to differences in the temperature dependence of the thermodynamic driving forces that govern order formation in the two systems. In crystal growth, the thermodynamic driving force increases exponentially with quench depth,¹ whereas in the case of block copolymers, the increase is approximately linear (see eq 4). Measurable growth rates during polymer crystallization are typically observed in melts that are supercooled 10–50 °C below T_{ODT} ,¹ whereas measurable grain growth rates in SI(20-6) required undercooling of 1 °C. The nature of the thermodynamic driving forces may also be responsible for this difference.

Although the factors that govern grain growth kinetics in block copolymers appear to be reasonably well understood, little is known about the processes that lead to nucleation of the ordered phase. We hope to address this important issue in future work.

The authors thank H. Wang, M. Y. Chang, S. S. Patel, J. H. Lee, and H. Hahn for their help during the early stages of this project. Financial support provided by the National Science Foundation (DMR-9901951 and DMR-9975592) and the Dreyfus Foundation is gratefully acknowledged. The small-angle neutron scattering instrument at the National Institute of Standards and Technology (NIST) is supported by the National

Science Foundation (DMR-9986442); NIST does not necessarily endorse the products and chemicals named in this article.

REFERENCES AND NOTES

1. Strobl, G. *The Physics of Polymers*; Springer: New York, 1997.
2. Porter, D. A.; Easterling, K. E. *Phase Transformations in Metals and Alloys*; Chapman & Hall: New York, 1992.
3. Ferry, J. D. *Viscoelastic Properties of Polymers*; Wiley: New York, 1980.
4. Leibler, L. *Macromolecules* 1980, 13, 1602.
5. Fredrickson, G. H.; Helfand, E. *J Chem Phys* 1987, 87, 697.
6. Fredrickson, G. H.; Binder, K. *J Chem Phys* 1989, 91, 7265.
7. Goveas, J. L.; Milner, S. T. *Macromolecules* 1997, 30, 2605.
8. Qi, S.; Wang, Z. G. *Phys Rev Lett* 1996, 76, 1679.
9. Rosedale, J. H.; Bates, F. S. *Macromolecules* 1990, 23, 2329.
10. Floudas, G.; Vlassopoulos, D.; Pitsikalis, M.; Hadjichristidis, N.; Stamm, M. *J Chem Phys* 1996, 104, 2083.
11. Sakamoto, N.; Hashimoto, T. *Macromolecules* 1998, 31, 3292.
12. Balsara, N. P.; Garetz, B. A.; Newstein, M. C.; Bauer, B. J.; Prosa, T. J. *Macromolecules* 1998, 31, 7668.
13. Balsara, N. P.; Perahia, D.; Safinya, C. R.; Tirrell, M.; Lodge, T. P. *Macromolecules* 1992, 25, 3896.
14. Balsara, N. P.; Garetz, B. A.; Dai, H. J. *Macromolecules* 1992, 25, 6072.
15. Dai, H. J.; Balsara, N. P.; Garetz, B. A.; Newstein, M. C. *Phys Rev Lett* 1996, 77, 3677.
16. Newstein, M. C.; Garetz, B. A.; Balsara, N. P.; Chang, M. Y.; Dai, H. J. *Macromolecules* 1998, 31, 64.
17. Balsara, N. P.; Garetz, B. A.; Chang, M. Y.; Dai, H. J.; Newstein, M. C.; Goveas, J. L.; Krishnamoorti, R.; Rai, S. *Macromolecules* 1998, 31, 5309.
18. Kim, W. G.; Chang, M. C.; Garetz, B. A.; Newstein, M. C.; Balsara, N. P.; Lee, J. H.; Hahn, H.; Patel, S. S. *J Chem Phys* 2001, 114, 10196.
19. Wang, H.; Newstein, M. C.; Chang, M. Y.; Balsara, N. P.; Garetz, B. A. *Macromolecules* 2000, 33, 3719.
20. Bates, F. S.; Schulz, M. F.; Khandpur, A. K.; Forster, S.; Rosedale, J. H.; Almdal, K.; Mortensen, K. *Faraday Discuss* 1994, 98, 7.
21. Lin, C. C.; Jonalagadda, S. V.; Kesani, P. K.; Dai, H. J.; Balsara, N. P. *Macromolecules* 1994, 27, 7769.
22. The discontinuity in $\phi(t)$ at $t = 80$ min is an experimental artifact, as discussed in ref. 18. It occurs at the time when the depolarized light scattering signal exceeds the dynamic range of the detector. This requires placing a neutral density filter in the optical path. We attempted to eliminate this discontinuity but were unsuccessful.
23. He, Y.; Oliver, B.; Ackerson, B. J. *Langmuir* 1997, 13, 1408.